Universal scaling laws of chaotic escape in dissipative multistable systems subjected to autoresonant excitations

Ricardo Chacón
Departamento de Física Aplicada, Escuela de Ingenierías Industriales, Universidad de Extremadura, Apartado Postal 382, E-06071 Badajoz, Spain
(Dated: June 4, 2009)

A theory concerning the emergence and control of chaotic escape from a potential well by means of autoresonant excitations is presented in the context of generic, dissipative, and multistable systems. Universal scaling laws relating both the onset and lifetime of transient chaos with the parameters of autoresonant excitations are derived theoretically using vibrational mechanics, Melnikov analysis, and energy-based autoresonance theory. Numerical experiments show that these scaling laws are robust against both the presence of noise and driving re-shaping.

PACS numbers: 05.45.Gg, 33.80.Gj

Introduction.−Escape from a potential well is an old problem with wide-ranging implications where the interplay of noise, dissipation, deterministic driving, and quantum uncertainty has given rise to unexpected and intriguing phenomena such as coherent destruction of tunneling [1] and stochastic resonance [2]. Other specific examples are pulse-shape-controlled tunneling [3], shot-noise-driven escape in Josephson junctions [4], and thermally induced escape [5]. While most previous investigations on driven escape have restricted themselves to purely periodic drivings, chirped excitations also have a demonstrated effectiveness. Chirped lasers, for example, can reduce the intensity required for infrared multiphoton dissociation of diatomic molecules to an experimentally realizable intensity range [6]. And chirped optical pulses have been shown to enhance charge flow in molecular-tunneling junctions [7]. In spite of the importance of chirped excitations [8], to the best of the author's knowledge, laws governing (some of) the associated escape scenarios remain to be revealed. The key to understanding the aforementioned effectiveness of chirped excitations is essentially the autoresonance (AR) mechanism: AR induced energy amplification in nonlinear, driven, and deterministic systems occurs when the system continuously adjusts its amplitude so that its instantaneous nonlinear period matches the instantaneous driving period of the chirped excitation. Initially studied in the context of a Hamiltonian description, AR phenomena have been well known for about half a century and have been observed in particle accelerators, planetary dynamics, atomic and molecular physics, and nonlinear oscillators [9], to cite a few examples. Regarding dissipative systems, an energy-based AR (EBAR) theory has recently been proposed and applied to the case where the system crosses a separatrix associated with its underlying integrable counterpart [10]. Since in such an escape situation the appearance of transient chaos associated with the occurrence of homoclinic bifurcations is an ubiquitous phenomenon, the question naturally arises: How does AR control the chaotic escape scenario, i.e., the onset and lifetime of transient chaos in generic dissipative multistable systems?

Theory.−In this Letter, this fundamental problem is studied in the context of the family of systems

$$\ddot{x} + dU/dx = -\delta\dot{x} + \gamma\sin\left[\Omega\left(t\right)t\right], \qquad (1)$$

where $U(x)$ is a generic multistable potential (see Fig. 1), and $\Omega\left(t\right) \equiv \omega + \alpha_n t^n, n = 1, 2, ...$, is a time-dependent frequency with α_n being the n-th-order sweep rate. One expects [10] $\gamma\sin\left[\Omega\left(t\right)t\right]$ to behave as an effective autoresonant excitation whenever the sweep rate is sufficiently low (adiabatic regime), which is the case considered throughout the present paper in order to apply Melnikov analysis (MA) to autoresonant excitations [11]. Also, the damping and autoresonant excitation terms are taken to be small amplitude perturbations of the underlying integrable system so as to deduce analytical expressions for the scaling laws relating both the onset time t_i and lifetime τ of transient chaos with the parameters of the AR excitation from the MA [12] results. The application of MA to any homoclinic (or heteroclinic) orbit $\left[x_{h,j}\left(t\right), \dot{x}_{h,j}\left(t\right)\right]$ of the unperturbed ($\delta = \gamma = 0$) counterpart of Eq. (1) involves calculating the corresponding Melnikov function (MF)

$$M_j\left(t_0\right) = -D + \gamma R_0\left(\omega, t_0\right) + \gamma\alpha_n R_1\left(\omega, t_0\right) + O\left(\gamma\alpha_n^2\right), \qquad (2)$$

where $D \equiv \delta\int_{-\infty}^{\infty}\dot{x}_{h,j}^2\left(t\right)dt > 0$, $R_0\left(\omega, t_0\right) \equiv \int_{-\infty}^{\infty}\dot{x}_{h,j}\left(t\right)\sin\left[\omega\left(t+t_0\right)\right]dt$, $R_1\left(\omega, t_0\right) \equiv \int_{-\infty}^{\infty}\left(t+t_0\right)^n\dot{x}_{h,j}\left(t\right)\cos\left[\omega\left(t+t_0\right)\right]dt$. For a purely periodic excitation ($\alpha_n = 0$), it is assumed in the following that the system does not exhibit transient chaos for a given set of parameter values, i.e., the MF (2) has no simple zeros:

$$D > \gamma\left|\max_{t_0\in\,\mathbb{R}} R_0\left(\omega, t_0\right)\right| \equiv \gamma A_0\left(\omega\right), \qquad (3)$$

where $A_0\left(\omega\right)$ represents a chaotic-threshold function whose generic behaviour is shown in Fig. 1. Indeed, homoclinic chaos is not possible for sufficiently small ω since a purely harmonic excitation becomes a constant when $\omega \rightarrow 0$. For sufficiently high ω, the dynamics can be analyzed using the vibrational mechanics approach [13] by separating $x(t) = z(t) + \psi\left(t\right)$,

FIG. 1: (color online) Generic multistable potential $U(x)$ vs x, and energy levels corresponding to different separatrices (dashed lines). The inset shows a generic chaotic threshold function $A_0(\omega)$ vs ω and the range $[\omega_{th,1}, \omega_{th,2}]$ in which homoclinic chaos is expected [see Eq. (3)].

where $z(t)$ represents the slow dynamics while $\psi(t)$ is the fast oscillating term: $\psi(t) = \psi_0 \cos(\omega t + \varphi_0)$ with $\psi_0 = \gamma\sqrt{\delta^2 + \omega^2}/\left(\omega\delta^2 - \omega^3\right)$, $\varphi_0 = \arctan(\delta/\omega)$. On averaging out $\psi(t)$ over time, the slow reduced dynamics of the system becomes

$$\ddot{z} + dV/dz = -\delta\dot{z}, \qquad dV/dz \equiv T^{-1}\int_0^T g\left[z + \psi_0 \cos(\omega t + \varphi_0)\right] dt, \tag{4}$$

where $g(x) \equiv dU(x)/dx, T \equiv 2\pi/\omega$, i.e., that of a *purely* damped system, and hence homoclinic chaos is not possible when $\omega \to \infty$. Note that this demonstrates that equilibria are the *only* attractors of the system for $\alpha_n > 0$. Thus, one concludes that the properties $A_0(\omega \to 0, \infty) = 0, A_0(\omega) \geqslant 0$ imply via the extreme value theorem (Weierstrass' theorem [14]) that the generic chaotic-threshold function $A_0(\omega)$ presents at least one maximum (the case shown in the inset of Fig. 1). Equation (2) indicates that the MF $M_j(t_0)$ has simple zeros (at sufficiently large values of t_0) for any positive value of the sweep rate because of the factor $(t + t_0)^n$ appearing in the definition of $R_1(\omega, t_0)$. Physically, this means that after a sufficiently long time, t_i, which depends upon the system's parameters and initial conditions, the instantaneous frequency of the autoresonant excitation reaches a threshold value $\Omega(t_i) = \omega_{th,1}$ that is the lowest frequency satisfying the relationship $D/\gamma = A_0(\omega_{th,1})$ (see Fig. 1, inset), i.e., the threshold condition for the onset of chaotic behaviour. It is worth noting that this occurs for any initial conditions because of the AR-induced increase of the system's energy. Thus, the condition $\Omega(t_i) = \omega_{th,1}$ implies the scaling law

$$t_i \sim (\omega_{th,1} - \omega)^{1/n} \alpha_n^{-1/n}, \tag{5}$$

for the onset time of transient chaos. Similarly, the lifetime τ of the chaotic transients can be estimated from the instantaneous frequency $\Omega(t_i + \tau) = \omega_{th,2}$ that is the lowest frequency satisfying the relationships $D/\gamma = A_0(\omega_{th,2}), \omega_{th,2} > \omega_{th,1}$ (see Fig. 1, inset), i.e.,

$$\tau \sim \left[(\omega_{th,2} - \omega)^{1/n} - (\omega_{th,1} - \omega)^{1/n}\right] \alpha_n^{-1/n}. \tag{6}$$

We see that the universal scaling laws (5) and (6) are *inverse-power* laws containing the two parameters (ω, α_n) that control the autoresonant excitation while the critical exponent is the inverse of the chirp order n. Notably, these scaling laws also contain the dependence upon the particular potential, initial potential well, and dissipation and excitation strengths through the threshold frequencies $\omega_{th,1}, \omega_{th,2}$. Since the mid 1980's, critical exponents of chaotic transients have been discussed theoretically in the context of crises in dissipative maps [15]. The present theory establishes that an inverse-power law remains valid also for dissipative multistable flows subjected to autoresonant excitations. The connection between such results for maps and the present ones can be readily understood by assuming that for a purely periodic excitation ($\alpha_n = 0$) there exists a chaotic attractor for a certain frequency ($\omega_{th,1} < \omega < \omega_{th,2}$) instead of a periodic attractor ($\omega_{th,1} > \omega$) (see Fig. 1, inset). According to the above discussion, the chaotic attractor disappears for $\alpha_n > 0$ via a boundary crisis and chaotic transients appear instead, with $\alpha = \alpha_{n,c} \equiv 0$ being the critical value for the crisis. Therefore, since the non-existence of simple zeros of the MF is a sufficient condition for the disappearance of transient chaos, the lifetime of these chaotic transients follows the universal inverse-power law

$$\tau \sim (\omega_{th,2} - \omega)^{1/n} \alpha_n^{-1/n}. \tag{7}$$

Now, applying EBAR theory one can deduce scaling laws relating both the onset time and lifetime with the autoresonant excitation amplitude. In particular, for Duffing-like potentials one has that the optimal amplitude scales as $\gamma \sim \left[3^n (n+1)!\right]^{3/(2n+2)} \alpha_n^{3/(2n+2)}$ [10] and hence the scaling law (7) for example becomes $\tau \sim \left[(\omega_{th,2} - \omega)(n+1)!\right]^{1/n} \gamma^{-(2n+2)/(3n)}$, where one sees that the critical exponent ranges from 4/3 for a linear chirp to 2/3 for the highest-order chirps.

Robustness vs noise and re-shaping.—Numerical experiments confirmed the accuracy of the above scaling laws in different systems. Representative results corresponding to a dimensionless Duffing oscillator $\ddot{x} = x - x^3 - \delta\dot{x} + \gamma\,\mathrm{sn}\left[2K(m)\Omega(t)\,t/\pi; m\right] + \sigma N(0,1)$ are shown in Figs. 2–5 for illustrative purposes. Here, $\mathrm{sn}(\cdot; m)$ is the Jacobian elliptic function of parameter $m \in [0,1]$ with $K(m)$ being the complete elliptic integral of the first kind. One has $\mathrm{sn}(\cdot; m=0) = \sin(\cdot)$ while, in the other limit, $\mathrm{sn}(\cdot; m=1)$ is the square-wave function [16]. Also, $\sigma N(0,1)$ is a white-noise term with $N(0,1)$ being a random variable with Gaussian distribution, zero mean, and variance 1, while $\sigma > 0$ controls the noise strength. For the purely deterministic ($\sigma = 0$) case of a sinusoidal ($m = 0$) excitation with a

linear chirp ($n = 1$), for example, and after calculating the resulting integrals by residues, one obtains the corresponding MF: $M^{\pm}_{Duffing}(t_0) = -D \mp B_0 \cos(\omega t_0) \mp \alpha_1 \left[B_1 t_0 \cos(\omega t_0) - \left(B_2 + B_0 t_0^2\right) \sin(\omega t_0)\right] + O\left(\gamma \alpha_1^2\right)$, where the sign $+(-)$ corresponds to the right (left) homoclinic orbit of the unperturbed Duffing oscillator ($\delta = \gamma = 0$), and $D \equiv 4\delta/3$, $B_0 \equiv \sqrt{2}\pi\gamma\omega \,\mathrm{sech}(\pi\omega/2)$, $B_1 \equiv 4\sqrt{2}\gamma \left[(\pi/2) - \left(\pi^2\omega/4\right) \tanh(\pi\omega/2)\right] \mathrm{sech}(\pi\omega/2)$, $B_2 \equiv \sqrt{2}\gamma \left(\pi^2/8\right) \mathrm{sech}^3(\pi\omega/2) \left[4\sinh(\pi\omega) - \pi\omega\cosh(\pi\omega) + 3\pi\omega\right]$. The results for the case of a periodic (chaotic) attractor existing at $\alpha_n = 0$ are shown in Fig. 2 (Fig. 4). While a linear chirp is considered in Figs. 2 and 3, Fig. 4 shows the results for quadratic and cubic chirps. Figures 2 and 4 show excellent agreement between numerical results and the predicted scaling laws for both the onset time and the lifetime of transient chaos. Figure 3(b) shows the AR-induced increase of energy over time until the separatrix energy level is reached, indicating the onset of transient chaos (see Figs. 3(a) and 3(d)), followed by a decrease of energy when the dynamics becomes effectively purely dissipative (see Fig. 3(c)). Note that the average energy remains roughly constant during transient chaos. The robustness of the scaling laws versus both the presence of additive noise and re-shaping of the autoresonant excitation is shown in Fig. 5. Note that, for the elliptic excitation, $\omega_{th,i}, i = 1, 2$, are functions of m, which is the reason for the different prefactors in the fits for $m = 0.995$ and $m = 1 - 10^{-14}$ (Fig. 5, bottom).

FIG. 2: (color online) Onset time (circles), t_i, and lifetime (squares, inset), τ, of transient chaos corresponding to a dimensionless Duffing oscillator (see the text) for $m = 0, \sigma = 0, \delta = 0.5, \gamma = 0.4$, and $\omega = 0.493$. Hence, $\omega_{th,2} = 1.11736, \omega_{th,1} = 0.49371$ from $M^{\pm}_{Duffing}(t_0)$ (see the text). Solid lines indicate fits according to the scaling laws (5) and (6), respectively.

FIG. 3: (color online) Autoresonant response of a dimensionless Duffing oscillator for a linear chirp $\alpha_1 = 3 \times 10^{-4}$ (see the text). (a) Position vs time and final equilibrium (dashed line). (b) Energy and average energy (over a few periods $2\pi/\omega$, thick black line) vs time. (c) Phase space trajectory and period-1 attractor existing at $\alpha_n = 0$ (thick black line). (d) Energy vs position (dashed line indicates the separatrix energy level as in version (b)). Remaining parameters are the same as in Fig. 2.

FIG. 4: (color online) Lifetime of transient chaos corresponding to a dimensionless Duffing oscillator (see the text) for quadratic ($n = 2$, squares) and cubic ($n = 3$, circles) chirps. Solid lines indicate fits according to the scaling law (7). Also shown is the chaotic attractor existing at $\alpha_{2,3} = 0$. Fixed parameters: $m = 0, \sigma = 0, \delta = 0.154, \gamma = 0.2, \omega = 1.1$. Hence, $\omega_{th,2} = 1.71404$ from $M^{\pm}_{Duffing}(t_0)$ (see the text).

Conclusions.—In sum, universal inverse-power laws relating both the onset and lifetime of transient chaos and

FIG. 5: (color online) Lifetime of transient chaos corresponding to a dimensionless Duffing oscillator (see the text) in the presence of noise (top panel, $m = 0, \gamma = 0.4$) and subjected to elliptic excitations (bottom panel, $\sigma = 0, \gamma = 0.3$). Solid lines indicate fits according to the scaling law (6). Fixed parameters: $\delta = 0.5, \omega = 0.493$.

the parameters of escape-inducing autoresonant excitations have been theoretically derived for generic, dissipative, and multistable flows. Numerical simulations showed the robustness of these scaling laws against both the presence of additive noise and driving re-shaping. Since the critical exponents were found to solely depend on the chirp's order, such scaling laws are expected to remain valid for even more general dissipative systems including spatiotemporal chaotic systems [17]. The present results can be readily tested experimentally (for example in mechanical and laser systems), and can find application to optimally control elementary dynamic processes characterized by chaotic escapes from a potential well, such as diverse atomic and molecular processes, transport phenomena in dissipative lattices, and control of the electron dynamics in quantum solid-state devices.

The author thanks Francisco Balibrea for stimulating discussions. Work partially supported by the Spanish MCyT through project FIS2008-01383.

[1] F. Grossmann *et al.*, Phys. Rev. Lett. **67**, 516 (1991).

[2] R. Benzi, A. Sutera, and A. Vulpiani, J. Phys. A **14**, L453 (1981); L. Gammaitoni *et al.*, Rev. Mod. Phys. **70**, 223 (1998).

[3] M. Holthaus, Phys. Rev. Lett. **69**, 1596 (1992).

[4] J. P. Pekola *et al.*, Phys. Rev. Lett. **95**, 197004 (2005).

[5] H. A. Kramers, Physica **7**, 284 (1940).

[6] S. Krempl *et al.*, Phys. Rev. Lett. **69**, 430 (1992).

[7] B. D. Fainberg, M. Jouravlev, and A. Nitzan, Phys. Rev. B **76**, 245329 (2007).

[8] For a recent review, see D. Goswami, Phys. Rep. **374**, 385 (2003).

[9] D. Bohm and L. Foldy, Phys. Rev. **70**, 249 (1946); R. Malhotra, Nature **365**, 819 (1993); J. Fajans and L. Friedland, Am. J. Phys. **69**, 1096 (2001); W. K. Liu, B. Wu, and J. M. Yuan, Phys. Rev. Lett. **75**, 1292 (1995).

[10] R. Chacón, Europhys. Lett. **70**, 56 (2005); Phys. Rev. E **78**, 066608 (2008).

[11] Notice that optimal (exact) autoresonance excitations are generally nonperiodic and unbounded [10], while MA remains valid for nonperiodic temporal perturbations if they are bounded; see, e.g., M. Taki, Phys. Rev. B **35**, 3267 (1987).

[12] V. K. Melnikov, Trans. Moscow Math. Soc. **12**, 1 (1963); J. Guckenheimer and P. J. Holmes, *Nonlinear Oscillations, Dynamical Systems and Bifurcation of Vector Fields* (Springer-Verlag, Berlin, 1983).

[13] I. I. Bleckman, *Vibrational Mechanics* (World Scientific, Singapore, 2000).

[14] See, e.g., H. J. Keisler, *Elementary Calculus. An Infinitesimal Approach* (Weber & Schmidt, Boston, 1986).

[15] C. Grebogi, E. Ott, and J. A. Yorke, Phys. Rev. Lett. **57**, 1284 (1986); K. T. Alligood, E. Sander, and J. A. York, Phys. Rev. Lett. **96**, 244103 (2006), and references therein.

[16] Note that, with the instantaneous period constant, solely the excitation shape is varied by increasing m from 0 to 1, and there is thus a smooth transition from a sine function to a square wave.

[17] E. L. Rempel and A. C.-L. Chian, Phys. Rev. Lett. **98**, 014101 (2007); J. Peixinho and T. Mullin, Phys. Rev. Lett. **96**, 094501 (2006).

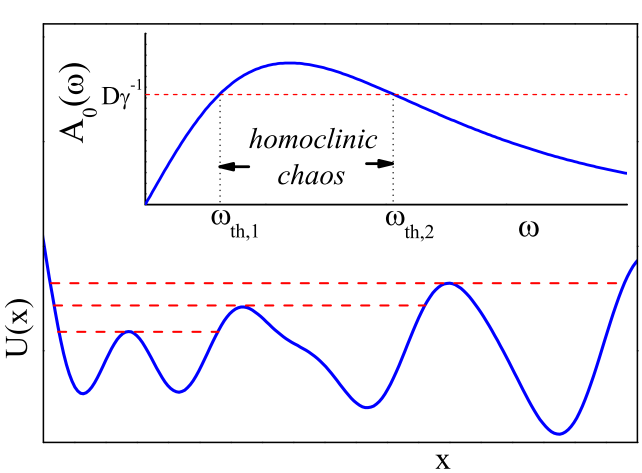

$A_0(\omega)$
$D\gamma^{-1}$
homoclinic
chaos
$\omega_{th,1}$
$\omega_{th,2}$
ω
U(x)
x

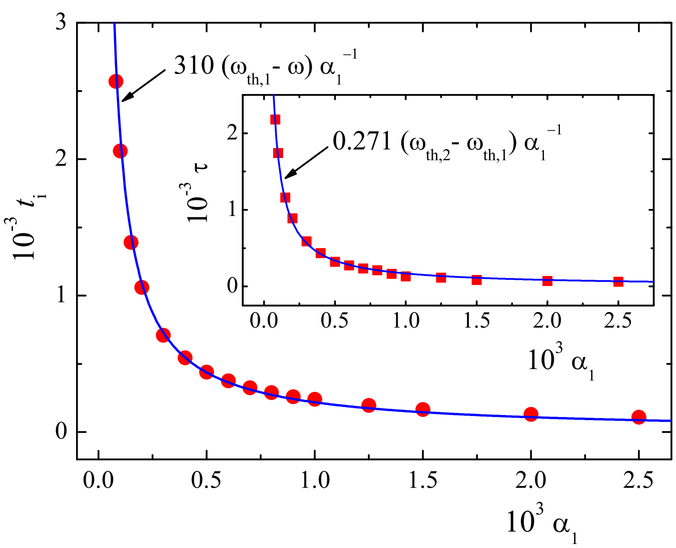

310 (ω_th,1 - ω) α_1^-1
0.271 (ω_th,2 - ω_th,1) α_1^-1
10^-3 t_i
10^-3 τ
10^3 α_1
0.0
0.5
1.0
1.5
2.0
2.5
0
1
2
3

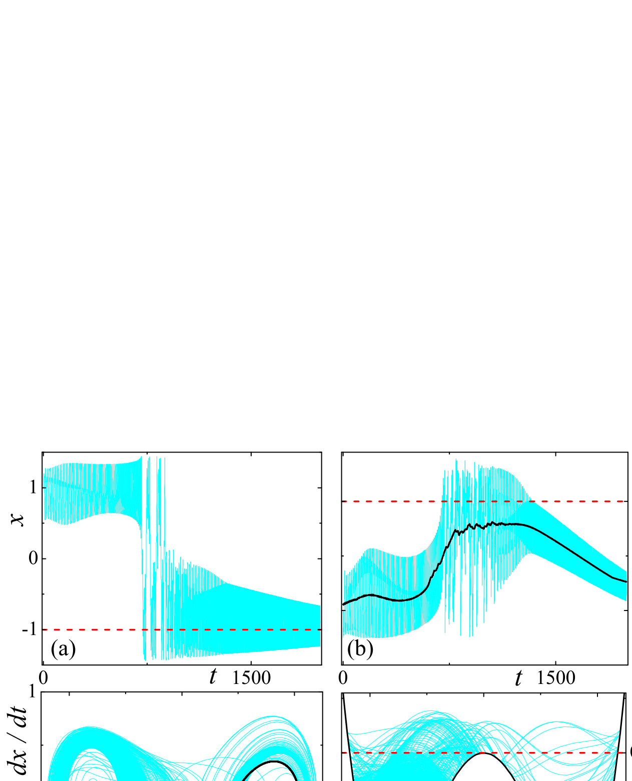

x
1
0
-1
(a)
0
t
1500
0.0
E
-0.2
(b)
0
t
1500
dx / dt
1
0
-1
(c)
-1.2
0.0
x
1.2
0.0
E
-0.2
(d)
-1.2
0.0
x
1.2

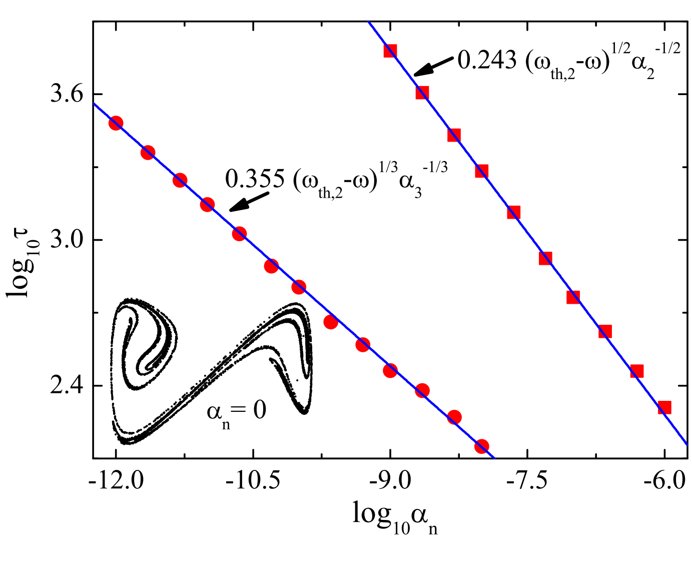

$0.243\ (\omega_{th,2}\text{-}\omega)^{1/2}\alpha_2^{-1/2}$
$0.355\ (\omega_{th,2}\text{-}\omega)^{1/3}\alpha_3^{-1/3}$
$\alpha_n = 0$
3.6
3.0
2.4
$\log_{10}\tau$
-12.0
-10.5
-9.0
-7.5
-6.0
$\log_{10}\alpha_n$

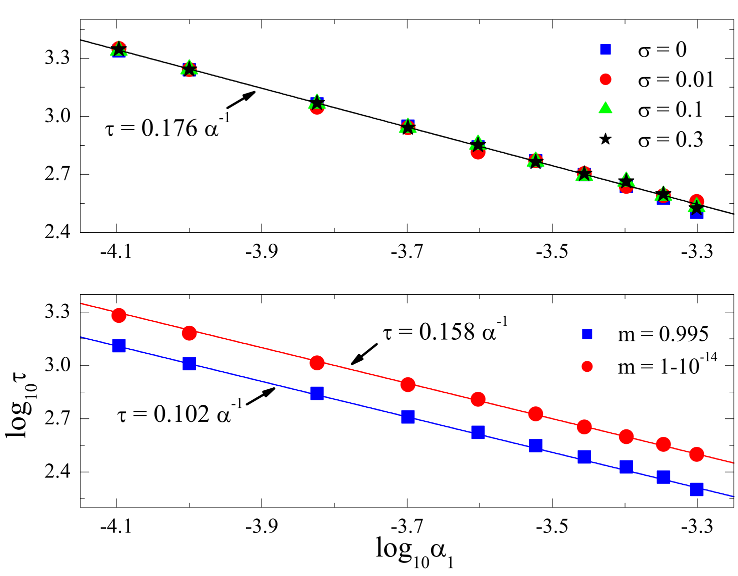

3.3
3.0
2.7
2.4
-4.1
-3.9
-3.7
-3.5
-3.3
σ = 0
σ = 0.01
σ = 0.1
σ = 0.3
τ = 0.176 α^-1
τ = 0.158 α^-1
τ = 0.102 α^-1
m = 0.995
m = 1-10^-14
log10τ
log10α1